I&EC research
Industrial & Engineering Chemistry Research

Article

pubs.acs.org/IECR

Application of Entransy Analysis in Self-Heat Recuperation Technology

Jing Wu*,† and Zeng Yuan Guo‡

†School of Energy and Power Engineering, Huazhong University of Science & Technology, Wuhan 430074, China

‡Key Laboratory for Thermal Science and Power Engineering of Ministry of Education, Department of Engineering Mechanics, Tsinghua University, Beijing 100084, China

ABSTRACT: Aside from the introductory and concluding remarks, this article is divided into four sections. Following a brief description of the concepts of entransy and entransy dissipation, which measures the irreversibility of heat transfer not related to heat-to-work conversion, a temperature−heat-flow-rate diagram ($T-\dot{Q}$ diagram) is applied to evaluate the heat-transfer irreversibility graphically, which can be used to reflect the performance of self-heat recuperation technology (SHRT) in chemical engineering. The entransy analyses in terms of temperature−heat-flow-rate diagrams for the chemical processes with gas and vapor/liquid streams show that a lower entransy-dissipation rate corresponds to better heat-recovery performance. Finally, both the quantitative entransy and exergy analyses indicate that, compared to the conventional self-heat exchange process, a process with SHRT achieved by changing the pressure of the effluent stream with a compressor provides much higher heat recovery and much lower energy requirement because of the much lower heat-transfer irreversibility measured by the entransy-dissipation rate or exergy-destruction rate. In addition, the differences between the entransy and exergy analyses are also discussed.

1. INTRODUCTION

Effective energy utilization, which aims to reduce energy consumption, has attracted significant attention because of concerns about a worldwide energy shortage. Improving heat-transfer performance is an important way to reduce energy consumption because nearly 80% of energy utilization is related to heat transfer. The chemical industry is a very large consumer of energy that uses a large number of heat-transfer processes, so improving their performance is critical to energy savings for the industry.

In the late 1970s, against the background of the then-current energy crisis,[1] pinch technology emerged as a tool for the design of heat-exchanger networks, which, as a method for using energy efficiently, aims to achieve financial savings by better process heat integration, maximizing heat recovery and reducing external utility loads. This technology is applicable to both single-stream and multistream processes.[2] However, a conventional heat-recovery process based on pinch technology has the limitation that the process heat cannot be completely recovered and additional heating and cooling loads are still needed in practical processes.[3]

To resolve this issue, Kansha et al.[4] developed self-heat recuperation technology (SHRT) based on exergy recuperation. Using SHRT, the reactor effluent stream is compressed by a compressor and exchanged with the reactor feed stream. As a result, the heat of the process stream can be circulated without heat addition, leading to a better energy-saving effect than can be achieved using a conventional heat-recovery approach based on pinch technology. So far, SHRT has been used in several industrial application cases including separation,[5,6] drying,[7,8] and CO_2 absorption[9] processes.

Recently, the new physical quantity of entransy has been introduced to describe the heat-transfer capacity of an object during a time period.[10] The entransy-dissipation rate rather than the entropy-generation rate or exergy-destruction rate can be used to measure the irreversibility of heat-transfer processes not involved in thermodynamic cycles for heat−work conversion.[11−14] Furthermore, the entransy-dissipation extremum principle has been proposed for the optimization of heat-transfer processes.[10,14]

In most chemical processes using conventional heat-recovery approaches or processes with SHRT, the objective of a heat-transfer process is only feed-stream heating or effluent-stream cooling, not heat−work conversion. Therefore, the entransy theory[14] should be applied to analyze SHRT. The contribution of this present article is to propose a simple and practical approach to evaluate the heat-transfer performances of chemical processes with recuperation technologies based on the concept of entransy dissipation.

2. ENTRANSY AND ENTRANSY DISSIPATION

The minimum-entropy-generation principle was presented by Bejan[15,16] for the optimization of heat-transfer performance, which is called thermodynamic optimization. This principle has been widely used to optimize the performance of various heat-transfer devices[17−20] based on the idea that the entropy generation is a measurement of irreversibility for any irreversible transport processes. However, the applicability of this principle to the optimization of heat-transfer processes has been called into question by some researchers.[21−25] For instance, Bertola and Cafaro[21] found that, when the Onsager reciprocal relation is satisfied, the principle of minimum entropy generation is tenable only if there is zero generalized

Received: September 23, 2013
Revised: November 27, 2013
Accepted: November 28, 2013

   dx.doi.org/10.1021/ie4031506 | Ind. Eng. Chem. Res. XXXX, XXX, XXX−XXX

flow under a nonzero generalized force. Chen et al.[11] and Finlayson[22] indicated that the heat-conduction equation can be driven from the minimum-entropy-generation principle only if the thermal conductivity is inversely proportional to the square of the absolute temperature. In reality, however, the thermal conductivity of most materials used in engineering is independent of temperature under normal conditions. Moreover, in a study of balanced counterflow heat exchangers, the heat-exchanger effectiveness in the range of 0−0.5 was increased, not decreased, with increasing entropy-generation number,[23] which is referred to as the "entropy-generation paradox". In addition, Shah and Skiepko[24] found that the effectiveness of heat exchangers with 18 different flow types can be a maximum, minimum, or intermediate value when the entropy-generation number attains extrema, all depending on the flow arrangement of the two fluids; that is, the entropy-generation minimization is not a general criterion of irreversibility for various kinds of heat exchangers. Because the exergy destruction, I, is proportional to entropy generation, S_g, according to the expression $I = T_0 S_g$, where T_0 is the environmental temperature, the minimum-exergy-destruction principle is not applicable to the analysis and optimization of some pure heat-transfer processes either. Investigating the reason for this discrepancy, it can be found that entropy generation or, equivalently, exergy destruction measures the loss of heat−work conversion ability. Either the minimum entropy generation or the minimum exergy destruction corresponds to the minimum loss of ability to do useful work. For some heat-transfer problems, however, the quantity of interest is the heat-transfer rate or coefficient rather than the heat−work conversion efficiency.[11−14]

Because entropy is not suitable for evaluating the irreversibility of such heat-transfer problems, a new physical quantity is needed to measure the irreversibility of heat-transfer problems that are not related to heat−work conversion. It is known that heat and electrical conduction processes are analogous because of the analogy between Fourier's law of heat conduction and Ohm's law of electrical conduction, where the heat flow corresponds to the electrical current and the thermal potential (i.e., the temperature) corresponds to the electrical potential. The analogies between the parameters for heat and electrical conduction processes are listed in ref 10, where it can be seen that the thermal system lacks a parameter that corresponds to the electrical potential energy of a capacitor. Hence, Guo et al.[10] defined the physical quantity G_{cm} for an incompressible object as

$$G_{cm} = \frac{1}{2}UT = \frac{1}{2}Mc_V T^2 \tag{1a}$$

where c_V is the specific heat capacity at constant volume, which is independent of temperature, T; M is the mass; U is the internal energy of the incompressible object; and G_{cm} is a state quantity called entransy, which was also referred to as the heat-transport potential capacity in an earlier article.[25] The physical meaning of G_{cm} is the heat-transfer capacity of an incompressible closed system during a time period, where the subscript cm denotes control mass. When the properties of the system are not uniform, the entransy of the system can be determined by integration as

$$G_{cm} = \int_V \frac{1}{2}\rho c_V T^2 \, dV \tag{1b}$$

where V is the volume of the system and ρ is the density. Note that, for an incompressible object with a temperature-dependent specific heat capacity, the entransy expression becomes

$$G_{cm} = \int_0^U T \, dU = \int_0^T MTc_V \, dT \tag{1c}$$

or

$$G_{cm} = \int_V \int_0^T \rho T c_V \, dT \, dV \tag{1d}$$

For engineering calculations, the entransy change during a heat-transfer process is of great interest, and the expressions for entransy in eqs 1a and 1b can be used with reasonable accuracy if the temperature range of the heat-transfer process is sufficiently small that c_V can be taken as a constant.

For heat-conduction problems in a closed system without reference to any work process and without any heat source, the energy conservation equation is

$$\frac{dU}{dt} = \dot{Q} \tag{2a}$$

where t is the time and $\dot{Q}$ is the heat-transfer rate. Equation 2a can be rewritten per unit of system volume as

$$\rho c_V \frac{\partial T}{\partial t} = -\nabla \cdot \dot{q} \tag{2b}$$

where ρ is the density and $\dot{q}$ is the heat flux. Multiplication of eq 2b by temperature, T, gives[10]

$$\rho c_V T \frac{\partial T}{\partial t} = -\nabla \cdot (\dot{q}T) + \dot{q} \cdot \nabla T \tag{3a}$$

Integrating eq 3a over the whole volume of the closed system, we obtain the entransy balance equation as

$$\int_V \left(\rho c_V T \frac{\partial T}{\partial t}\right) dV = \int_V -\nabla \cdot (\dot{q}T) \, dV + \int_V (\dot{q} \cdot \nabla T) \, dV \tag{3b}$$

Based on the expression for entransy in eq 1b, we have

$$\int_V \left(\rho c_V T \frac{\partial T}{\partial t}\right) dV = \frac{dG_{cm}}{dt} \tag{4a}$$

Furthermore, Gauss's theorem gives

$$\int_V -\nabla \cdot (\dot{q}T) \, dV = \int_S -(\dot{q}T) \cdot \vec{n} \, dS \tag{4b}$$

where S is the boundary surface of the closed system. Substituting eqs 4a and 4b and Fourier's law, $\dot{q} = -k\nabla T$, into eq 3b, gives the entransy balance equation

$$\frac{dG_{cm}}{dt} = \int_S -(\dot{q}T) \cdot \vec{n} \, dS - \int_V k(\nabla T)^2 \, dV \tag{3c}$$

where k is the thermal conductivity. The left side of eq 3c is the time variation of the entransy stored in the closed system. The first term on the right is the entransy-transfer rate associated with heat transfer across the system boundary, whereas the second term on the right is the total entransy-dissipation rate within the system boundary, which resembles the electrical energy dissipation rate in an electrical system and the mechanical energy dissipation rate in viscous fluid flow.[10,14,26] Equations 2a and 3c indicate that, during a heat-transfer process

dx.doi.org/10.1021/ie4031506 | Ind. Eng. Chem. Res. XXXX, XXX, XXX−XXX

without volume variation, heat is conserved whereas entransy is nonconserved but rather is dissipated due to the irreversibility.

The expressions for entransy in eqs 1a−1d are valid for closed systems, whereas for open systems involving mass flow such as in a heat exchanger, the entransy of a flowing fluid (denoted by G_{cv}) becomes

$$G_{cv} = \frac{1}{2}HT = \frac{1}{2}mc_pT^2 \tag{5}$$

where c_p is the specific heat capacity at constant pressure independent of temperature, T; H is the enthalpy of the flowing fluid; and G_{cv} is a state quantity called the enthalpy entransy.[27] It is worth noting that the notation, G, in this article represents the entransy of an object and should not be confused with the Gibbs free energy.

For heat transfer in a two-fluid heat exchanger with an arbitrary flow arrangement, the heat-transfer rate between the hot and cold fluids over a differential element is

$$d\dot{Q} = -\dot{m}_h\, dh_h = \dot{m}_c\, dh_c \tag{6}$$

where $\dot{m}$ is the mass flow rate; h is the specific enthalpy; and the subscripts h and c denote the hot and cold fluids, respectively.

If the specific heat capacities of the fluids at constant pressure, $c_{p,h}$ and $c_{p,c}$, are constant, eq 6 can be rewritten as

$$d\dot{Q} = -\dot{m}_h c_{p,h}\, dT_h = \dot{m}_c c_{p,c}\, dT_c \tag{7}$$

Multiplying both sides of eq 7 by T_h and T_c yields[26]

$$d\dot{G}_h = -T_h\, d\dot{Q} \tag{8a}$$

$$d\dot{G}_c = T_c\, d\dot{Q} \tag{8b}$$

where $\dot{G}_h = {}^1/_2\dot{m}_h c_{p,h} T_h{}^2$ is the enthalpy entransy of the flowing hot fluid with mass flow rate $\dot{m}_h$ and $\dot{G}_c = {}^1/_2\dot{m}_c c_{p,c} T_c{}^2$ is the enthalpy entransy of the flowing cold fluid with mass flow rate $\dot{m}_c$. Note that, for simplicity of notation, we drop the subscript cv denoting the control volume from G_{cv} in this remainder of the article. The left-hand side in eq 8a or 8b is the change in enthalpy entransy of the hot or cold fluid, respectively, and the right-hand side is the local entransy-transfer rate out of the hot fluid associated with heat-transfer rate $d\dot{Q}$ at T_h or that into the cold fluid associated with $d\dot{Q}$ at T_c, respectively.[26]

By integrating eqs 8a and 8b over the total heat-transfer rate, we obtain

$$\dot{G}_{h,out} - \dot{G}_{h,in} = \int_0^{\dot{Q}_t} -T_h\, d\dot{Q} \tag{9a}$$

$$\dot{G}_{c,out} - \dot{G}_{c,in} = \int_0^{\dot{Q}_t} T_c\, d\dot{Q} \tag{9b}$$

where the subscripts in and out denote the inlet and outlet states, respectively, of the hot and cold fluids and $\dot{Q}_t$ is the total heat-transfer rate between the hot and cold fluids.

The entransy-dissipation rate in the heat exchanger due to heat transfer from the hot fluid to the cold fluid can be obtained by summing eqs 9a and 9b[26]

$$\begin{aligned}\dot{G}_\phi &= (\dot{G}_{h,in} + \dot{G}_{c,in}) - (\dot{G}_{h,out} - \dot{G}_{c,out}) \\ &= \left(\frac{1}{2}\dot{m}_h c_{p,h} T_{h,in}{}^2 + \frac{1}{2}\dot{m}_c c_{p,c} T_{c,in}{}^2\right) \\ &\quad - \left(\frac{1}{2}\dot{m}_h c_{p,h} T_{h,out}{}^2 + \frac{1}{2}\dot{m}_c c_{p,c} T_{c,out}{}^2\right) \\ &= \int_0^{\dot{Q}_t} (T_h - T_c)\, d\dot{Q}\end{aligned} \tag{10}$$

where $\dot{G}_\phi$ is the entransy-dissipation rate.

Chen et al.[14] enumerated the differences between entransy theory and entropy theory for optimization. Depending on two different purposes, various heat-transfer problems have two different irreversibility measures for process optimization. When the transferred heat is for heat−work conversion, the entropy-generation rate is the best measure of irreversibility, and optimization should involve application of the minimum-entropy-generation (-exergy-destruction) principle, whereas when the transferred heat is for object heating or cooling only, the entransy-dissipation rate is the best measure of irreversibility, and the extremum-entransy-dissipation principle should be applied for optimization. Use of these different principles to optimize the same heat-transfer process will lead to different optimization results.

The extremum-entransy-dissipation principle has been applied to the optimization of several types of heat-transfer processes not involved in thermodynamic cycles, including heat conduction, convection, and radiation.[10−14,28,29] Based on theoretical analyses, a few heat-transfer enhancement approaches and technologies have been developed, such as the use of discrete double inclined rib tubes and alternating elliptical axis tubes.[14] Entransy-dissipation-based thermal resistance is, in fact, the least action of a pure heat-transfer process,[11] from which Fourier's law with a constant thermal conductivity can be derived. Moreover, it was found that, unlike the nonmonotonic variation of the heat-exchanger effectiveness with the entropy-generation number, the dimensionless thermal resistance of a heat exchanger defined on the basis of the entransy-dissipation rate decreases monotonically with increasing effectiveness,[26] that is, no paradox occurs, showing that the entransy-dissipation rate is a preferable irreversibility measurement for heat-transfer processes with the purpose of object heating or cooling only.

3. TEMPERATURE−HEAT-FLOW-RATE DIAGRAM AND ITS PHYSICAL MEANING

In thermodynamics, property diagrams, such as $p-v$ and $T-s$ diagrams, have served as great visual aids in the analysis of thermodynamic processes. Such property diagrams can directly show the variation of the properties of a system during a reversible thermodynamic process. More importantly, the magnitudes of the expansion work and heat exchanged between the system and the surroundings of a reversible process can be represented by the areas under the process curves in $p-v$ and $T-s$ diagrams, respectively, providing a convenient approach for studying and understanding thermodynamic processes.

In heat transfer, the common diagram used to analyze the variation of fluid temperatures in a heat exchanger is the $T-A$ diagram, as shown in Figure 1a. A $T-A$ diagram consists of two axes, where the x axis represents the heat-exchange area and the y axis represents the temperature of the hot or cold fluid. The

dx.doi.org/10.1021/ie4031506 | Ind. Eng. Chem. Res. XXXX, XXX, XXX−XXX

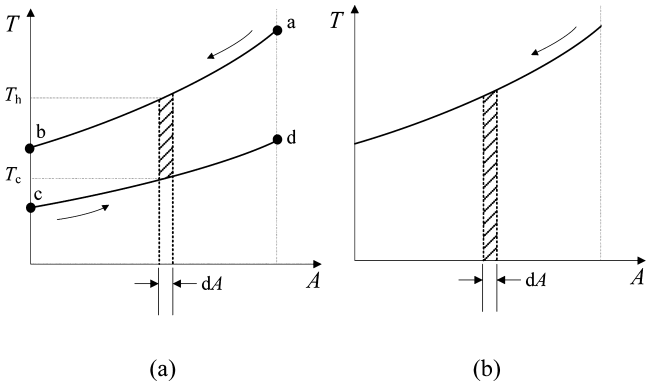

Figure 1. Variation of fluid temperatures with heat-transfer area in a counterflow heat exchanger: (a) patterned area is proportional to the heat-transfer rate, (b) patterned area is meaningless.

heat-transfer rate between the hot and cold fluids over a differential area, dA, is

$$d\dot{Q} = K(T_h - T_c)\, dA \tag{11}$$

where K is the overall heat-transfer coefficient of the heat exchanger and T_h and T_c are the temperatures of the hot and cold fluids, respectively, on the two sides of the differential area, dA, as shown in Figure 1a.

By integrating eq 11 from the inlet of the heat exchanger to its outlet, one can obtain the total heat-transfer rate between the hot and cold fluids in the heat exchanger, which is proportional to the quadrilateral area enclosed by the two curves of hot and cold fluids, that is, the area a−b−c−d shown in Figure 1a. Note that, although the area between the two curves in the T−A diagram corresponds to the total heat-transfer rate, the projected area of each curve on the x axis, as shown in Figure 1b, is meaningless. More importantly, there is no way to describe the heat-transfer irreversibility with the T−A diagram.[30]

Taking the temperature and the enthalpy change of the flowing hot or cold fluid in a heat exchanger as the y and x axes, respectively, one can construct a T−$\Delta\dot{H}$ ($\Delta\dot{H} = \dot{H}_{in} - \dot{H}$) diagram to represent the state changes of the hot and cold fluids, as illustrated in Figure 2. With a constant heat-capacity flow rate, that is, a constant product of the mass flow rate and the specific heat of the fluid, $\dot{m}c_p$, the temperature varies linearly with the enthalpy of the flowing fluid with a slope of $1/\dot{m}c_p$.

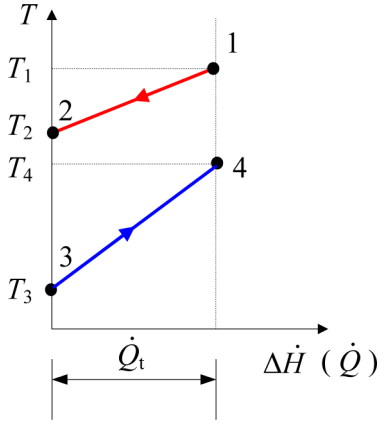

Figure 2. T−$\Delta\dot{H}$ diagram for the hot and cold fluids in a counterflow heat exchanger.

During the heat-transfer process, the total heat supplied by the hot fluid and obtained by the cold fluid is equal to the enthalpy change of each fluid, that is, $\dot{Q} = -\dot{m}_h\Delta h_h = \dot{m}_c\Delta h_c$ or $\dot{Q} = \Delta\dot{H}_h = \Delta\dot{H}_c$. Thus, the T−$\Delta\dot{H}$ diagram is usually referred to as the T−$\dot{Q}$ diagram.[4,30,31]

In fact, according to the energy conservation relation

$$\dot{Q} = \dot{m}_h h_{h,in} - \dot{m}_h h_h = \dot{m}_c h_c - \dot{m}_c h_{c,in} \tag{12}$$

when the inlet enthalpies of the hot and cold fluids, $\dot{m}_h h_{h,in}$ and $\dot{m}_c h_{c,in}$, respectively, are prescribed, the heat-transfer rate, $\dot{Q}$, corresponds to the enthalpy of the hot or cold fluid at any state, that is, $-\dot{m}_h h_h$ or $\dot{m}_c h_c$, during the heat-transfer process. Thus, the heat-transfer rate, $\dot{Q}$, that is, the horizontal ordinate in Figure 2, can be regarded as a state parameter of the flowing fluid.

Unlike on the T−A diagram, where the projected area of each curve on the x axis is meaningless and the heat-transfer irreversibility cannot be represented graphically, the projected area of each temperature line for the hot and cold fluids on the x axis and the area between them on the T−$\dot{Q}$ diagram have clear physical meanings thanks to the concept of entransy. The patterned area in Figure 3a is equal to T_h d$\dot{Q}$, which is the

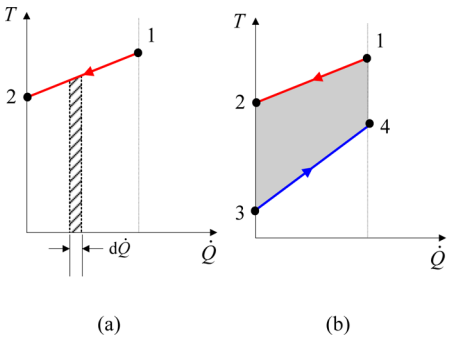

Figure 3. T−$\dot{Q}$ diagram of a counterflow heat exchanger: (a) patterned area is the differential entransy-transfer rate out of the hot fluid, (b) shaded area is the total entransy-dissipation rate.

differential entransy-transfer rate out of the hot fluid associated with heat-transfer rate d$\dot{Q}$ according to eq 8a. Thus, the total entransy-transfer rate out of the hot fluid during the entire heat-transfer process, as shown in eq 9a, can be obtained by adding all of the differential entransy-transfer rates, which is equal, in magnitude, to the total area under temperature line 1−2 of the hot fluid in the T−$\dot{Q}$ diagram. Similarly, the magnitude of the total entransy-transfer rate into the cold fluid is represented by the area under temperature line 3−4 of the cold fluid in the T−$\dot{Q}$ diagram. Therefore, the difference between these two areas, as represented by the shaded area in Figure 3b, is the total entransy-dissipation rate, $\dot{G}_\phi$, as shown in eq 10.[30]

Because the entransy-dissipation rate is a measurement of the irreversibility of heat-transfer processes not involved in thermodynamic cycles, T−$\dot{Q}$ diagrams can be used as valuable tools for visualizing heat-transfer performances. For instance,[30] it is well-known that the effectiveness of a counterflow heat exchanger is higher than that of a parallel-flow heat exchanger under the same heat load. Consider a given heat exchanger with a finite heat-transfer area, as in Figure 4a. In the case of counterflow, the area of trapezoid 1−2−3−4 shown in Figure 4b represents the entransy-dissipation rate of the heat-transfer process. If the flow pattern changes to parallel flow with the transferred heat and the inlet temperature of the hot fluid

dx.doi.org/10.1021/ie4031506 | Ind. Eng. Chem. Res. XXXX, XXX, XXX−XXX

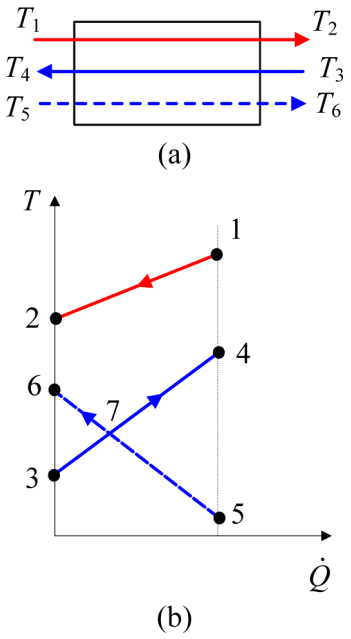

Figure 4. Counterflow and parallel-flow heat exchangers with the same heat load: (a) flow diagram, (b) $T-\dot{Q}$ diagram.

unchanged, the variation of the cold fluid temperature with the heat-transfer rate is shown by line 5−6 in Figure 4b. Note that, to transfer the same amount of heat as in the case of counterflow, the inlet temperature of the cold stream in the case of parallel flow drops from T_3 to T_5. As a result, the area of isosceles triangle 4−5−7 is larger than that of the isosceles triangle 3−6−7. This shows that the entransy-dissipation rate of the heat-transfer process in the counterflow heat exchanger is smaller than that in the parallel-flow heat exchanger, which leads to a higher effectiveness, that is, a better heat-transfer performance.

It might appear that the $T-\dot{Q}$ diagram discussed above is the same as the $T-\dot{Q}$ diagram used in both pinch technology and self-heat recuperation technology (SHRT),[3,4,31] but in fact, there are significant differences between them. First, without the concept of entransy, it was not possible to establish the relationship between the area in the $T-\dot{Q}$ diagram and the irreversibility of the heat-transfer process in previous studies of pinch technology or SHRT. Second, in pinch technology studies, a single hot composite curve of all hot streams and a single cold composite curve of all cold streams can be constructed in the $T-\dot{Q}$ diagram.[1,2,31] However, the area between the hot and cold composite curves cannot reflect the irreversibility of the multistream heat-transfer process because the area is no longer the entransy-dissipation rate. Third, in previous literature on pinch technology,[3,4,31] the $T-\dot{Q}$ diagram is referred to as a temperature−heat diagram even though the unit of the horizontal ordinate is not joules but watts, so that it should be called a temperature−heat-transfer-rate diagram. It is known from equilibrium thermodynamics that heat is a process quantity. In contrast, the heat-transfer rate, $\dot{Q}$, can be considered as a state quantity in heat transfer because it corresponds to the enthalpy of the flowing hot or cold fluid at any state when the inlet enthalpies of the hot and cold fluids are prescribed, as discussed above based on eq 12.

4. APPLICATION OF $T-\dot{Q}$ DIAGRAM IN SHRT

In this section, following a previous study of SHRT,[4] we present an analysis of irreversibility by using the $T-\dot{Q}$ diagram based on entransy theory. For consistency, we partially use the same notation as in ref 4. Moreover, the specific heat capacity of the hot or cold fluid at constant pressure is assumed to be constant for the sake of simplicity, as in ref 4.

4.1. Gas Stream. Simple chemical process I mentioned in ref 4 is shown in Figure 5a, where a gas stream is heated from

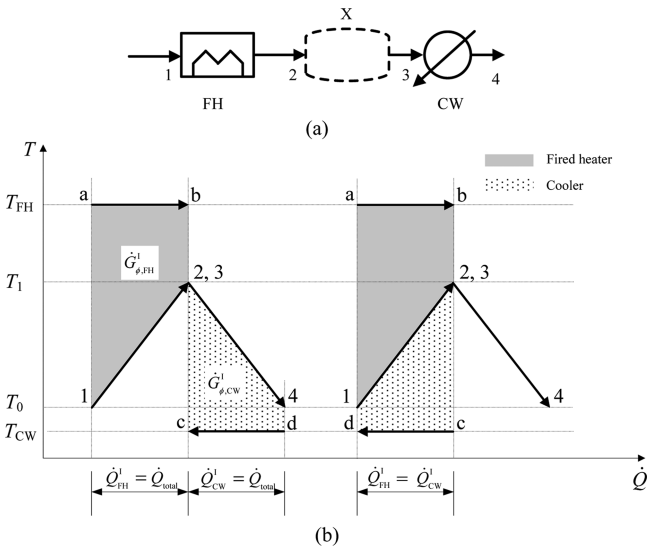

Figure 5. Simple thermal process I for the gas stream: (a) flow diagram;[4] (b) $T-\dot{Q}$ diagram, where the shaded and patterned areas together represent the entransy-dissipation rate.

temperature T_0 to a certain operating temperature T_1 of the following process X (e.g., reactor) by a fired heater (FH) and cooled to temperature T_0 by cooling water (CW) after process X. Figure 5b shows the $T-\dot{Q}$ diagram, where the shaded and patterned areas together represent the entransy-dissipation rate of this process.

If the temperatures of the gas stream before and after process X, namely, T_2 and T_3, are the same, the external heating load, $\dot{Q}^{I}_{FH}$, is equal to the external cooling load, $\dot{Q}^{I}_{CW}$, which can be written as[4]

$$\dot{Q}_{total} = \dot{Q}^{I}_{FH} = \dot{Q}^{I}_{CW} \tag{13}$$

where $\dot{Q}_{total}$ is the total heating duty of the fired heater or the cooler.

Assuming that the temperature of the fuel in FH, T_{FH}, is kept constant when it supplies heat to the gas stream during process 1−2, the entransy-dissipation rate of this heat-transfer process is

$$\begin{aligned}\dot{G}^{I}_{\phi,FH} &= \int_0^{\dot{Q}_{total}} (T_{FH} - T_g)\, d\dot{Q} \\ &= \dot{Q}_{total} T_{FH} - \left(\frac{1}{2}\dot{m}c_p T_1^2 - \frac{1}{2}\dot{m}c_p T_0^2\right)\end{aligned} \tag{14}$$

which is represented by the shaded area, $\dot{G}^{I}_{\phi,FH}$, in Figure 5b. In eq 14, the term $\dot{Q}_{total}T_{FH}$ is the entransy-transfer rate out of the fired heater, whereas the term $^1/_2\dot{m}c_pT_1^2 - {}^1/_2\dot{m}c_pT_0^2$ stands for the total enthalpy entransy obtained by the flowing gas stream with mass flow rate $\dot{m}$. Thus, the difference between these two

dx.doi.org/10.1021/ie4031506 | Ind. Eng. Chem. Res. XXXX, XXX, XXX−XXX

terms is the entransy-dissipation rate of heat-transfer process 1−2.

Similarly, if the temperature of CW, T_{CW}, is unchanged during cooling process 3−4, the entransy-dissipation rate during this process is given by

$$\dot{G}^{I}_{\phi,CW} = \int_0^{\dot{Q}_{total}} (T_g - T_{CW})\, d\dot{Q} = \left(\frac{1}{2}\dot{m}c_p T_1^2 - \frac{1}{2}\dot{m}c_p T_0^2\right) - \dot{Q}_{total}T_{CW} \quad (15)$$

as shown by the patterned area, $\dot{G}^{I}_{\phi,CW}$, in Figure 5b. In eq 15, the term $^1/_2\dot{m}c_pT_1^2 - {}^1/_2\dot{m}c_pT_0^2$ is the decreased enthalpy entransy of the flowing gas stream, and the term $\dot{Q}_{total}T_{CW}$ is the entransy-transfer rate into the cooling water.

Combining eqs 14 and 15, we obtain the total entransy-dissipation rate of simple chemical process I as

$$\dot{G}^{I}_{\phi,total} = \dot{G}^{I}_{\phi,FH} + \dot{G}^{I}_{\phi,CW} = \dot{Q}_{total}(T_{FH} - T_{CW}) \quad (16)$$

which is just the area of the rectangle a−b−c−d consisting of two trapezoids as shown in Figure 5b. Here, the letters a−d represent the four vertices of the rectangle. Because the entransy-dissipation rate measures the irreversibility of heat-transfer processes, it can be seen from Figure 5b that the irreversibility of simple chemical process I is very large because of the large temperature difference between the fired heater (>800 °C) and the cooling water (~25 °C).

Note that, for some cases (e.g., variable heat capacities or $T_2 \neq T_3$), heating line 1−2 and cooling line 3−4, as shown in Figure 5b, might not be symmetrical, in which case the rectangle cannot be obtained. However, for these conditions, the total entransy-dissipation rate can also be calculated by adding the areas between the hot and cold curves of each heat-transfer process in the $T-\dot{Q}$ diagram.

Figure 6a shows improved chemical process II, which uses a feed−effluent heat exchanger in which heat is exchanged between the feed and effluent streams to recirculate the self-heat of the streams.[4] Figure 6b shows the $T-\dot{Q}$ diagram, where the shaded and patterned areas together represent the entransy-dissipation rate of this process.

In the feed−effluent heat exchanger under the condition of a minimum temperature difference, ΔT_{min}, the feed stream is preheated in the heat exchanger from T_0 to T_2, and the effluent stream is cooled from T_1 to T_5. The feed stream is then heated by FH to the required temperature T_1, for process X, and the effluent stream is finally cooled to T_0 by CW. It can be seen in Figure 6b that[4]

$$\dot{Q}_{total} - \dot{Q}^{II}_{HX} = \dot{Q}^{II}_{FH} = \dot{Q}^{II}_{CW} \quad (17)$$

where $\dot{Q}^{II}_{HX}$ is the feed−effluent heat-exchanger duty and $\dot{Q}^{II}_{FH}$ and $\dot{Q}^{II}_{CW}$ are the external heating load and external cooling load, respectively.

The total entransy dissipation of process II, as shown in Figure 6b, consists of three parts, namely, the entransy dissipations during the heat-transfer processes in the fired heater (FH), in the feed−effluent heat exchanger (HX), and in the cooler (CW). They are represented by the three shaded or patterned areas $\dot{G}^{II}_{\phi,FH}$, $\dot{G}^{II}_{\phi,HX}$ and $\dot{G}^{II}_{\phi,CW}$, respectively, and their expressions can be derived from the trapezoid formula as

$$\dot{G}^{II}_{\phi,FH} = \left(T_{FH} - T_1 + \frac{1}{2}\Delta T_{min}\right)\dot{Q}^{II}_{FH} \quad (18)$$

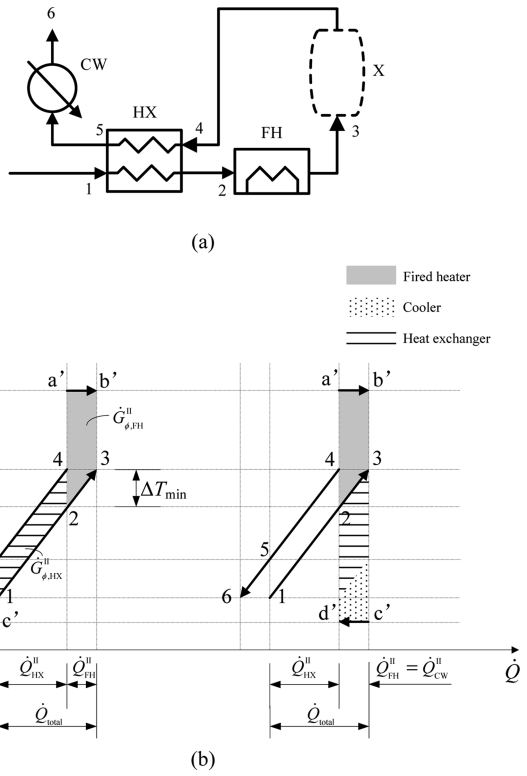

Figure 6. Improved thermal process II with a feed−effluent heat exchanger for the gas stream: (a) flow diagram;[4] (b) $T-\dot{Q}$ diagram, where the shaded and patterned areas together represent the entransy-dissipation rate.

$$\dot{G}^{II}_{\phi,HX} = \dot{Q}^{II}_{HX}\Delta T_{min} \quad (19)$$

$$\dot{G}^{II}_{\phi,CW} = \left(T_0 - T_{CW} + \frac{1}{2}\Delta T_{min}\right)\dot{Q}^{II}_{CW} \quad (20)$$

Summing the shaded and patterned areas in Figure 6b gives the total entransy-dissipation rate in chemical process II as

$$\dot{G}^{II}_{\phi,total} = \dot{G}^{II}_{\phi,FH} + \dot{G}^{II}_{\phi,HX} + \dot{G}^{II}_{\phi,CW} = \dot{Q}^{II}_{FH}(T_{FH} - T_{CW}) \quad (21)$$

which is just the area of the rectangle a′−b′−c′−d′ as shown in Figure 6b. It can be seen from eqs 16 and 21 that the entransy-dissipation rate of process II is dramatically decreased compared with that of process I because $\dot{Q}^{II}_{FH}$ is much smaller than $\dot{Q}_{total}$.

The total entransy-dissipation rates given by eqs 16 and 21 can also be calculated by taking overall chemical processes I and II, respectively. For process I, the entransy-transfer rate corresponding to the heat-transfer rate of the fired heater is $\dot{Q}^{I}_{FH}T_{FH}$, and the entransy-transfer rate corresponding to the heat-transfer rate of the cooling water is $\dot{Q}^{I}_{CW}T_{CW}$. The change in the entransy of the gas stream is zero because the inlet temperature (point 1) equals the outlet temperature (point 4). As a result, according to the entransy balance relation, the entransy dissipation of process I is $\dot{Q}^{I}_{FH}T_{FH} - \dot{Q}^{I}_{CW}T_{CW}$, the same expression as in eq 16 using $\dot{Q}^{I}_{FH} = \dot{Q}^{I}_{CW}$ in eq 13. For process II, the same analysis is also applicable.

Thermal process III of the gas stream for heat circulation using SHRT is shown in Figure 7a, where a compressor is used to provide perfect internal heat circulation.[4] Before entering the heat exchanger, the effluent stream is compressed adiabatically

dx.doi.org/10.1021/ie4031506 | Ind. Eng. Chem. Res. XXXX, XXX, XXX−XXX

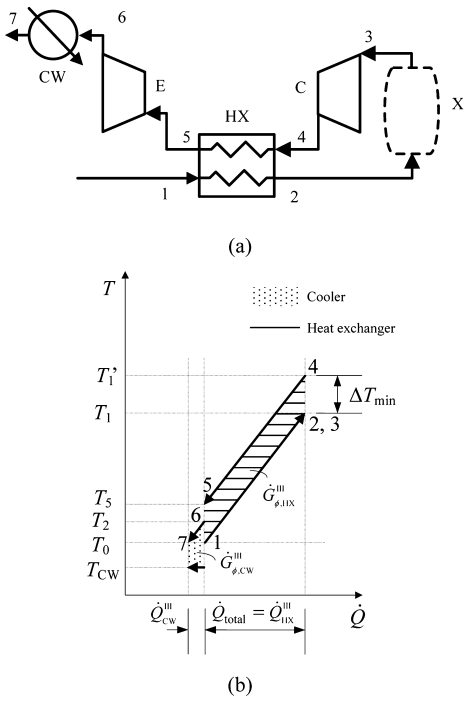

Figure 7. Thermal process III with SHRT for the gas stream: (a) flow diagram;[4] (b) $T-\dot{Q}$ diagram, where the patterned areas together represent the entransy-dissipation rate.

by a compressor to a higher temperature, T_1'. As a result, the total heating duty of the feed stream can be entirely provided by the effluent stream with the self-heat exchanger. Then, the effluent stream is adiabatically decompressed by an expander to recover part of the work of the compressor. Finally, the effluent stream is cooled to T_0 by cooling water. The shaft powers of the compressor and expander are denoted as $\dot{W}_c$ and $\dot{W}_E$, respectively.

The entransy-dissipation rate of process III comes from two heat-transfer processes with finite temperature differences, as shown by the patterned areas in Figure 7b, namely, the heat transfer in the feed−effluent heat exchanger (HX) and that in the cooler (CW). The corresponding expressions are

$$\dot{G}_{\phi,\mathrm{HX}}^{\mathrm{III}} = \dot{Q}_{\mathrm{total}}\Delta T_{\mathrm{min}} \tag{22}$$

and

$$\dot{G}_{\phi,\mathrm{CW}}^{\mathrm{III}} = \frac{1}{2}(T_0 + T_2 - 2T_{\mathrm{CW}})\dot{Q}_{\mathrm{CW}}^{\mathrm{III}} \tag{23}$$

Therefore, the total entransy-dissipation rate of the chemical process with SHRT is

$$\dot{G}_{\phi,\mathrm{total}}^{\mathrm{III}} = \dot{G}_{\phi,\mathrm{HX}}^{\mathrm{III}} + \dot{G}_{\phi,\mathrm{CW}}^{\mathrm{III}} = \dot{Q}_{\mathrm{total}}\Delta T_{\mathrm{min}} + \dot{Q}_{\mathrm{CW}}^{\mathrm{III}}\left(\frac{T_2 + T_0}{2} - T_{\mathrm{CW}}\right) \tag{24}$$

For further analysis, the total entransy-dissipation rate of process II is rewritten as

$$\dot{G}_{\phi,\mathrm{total}}^{\mathrm{II}} = \dot{Q}_{\mathrm{total}}\Delta T_{\mathrm{min}} + \dot{Q}_{\mathrm{CW}}^{\mathrm{II}}(T_{\mathrm{FH}} - T_{\mathrm{CW}} + T_0 - T_1) \tag{25}$$

Subtracting eq 25 from eq 24 gives

$$\dot{G}_{\phi,\mathrm{total}}^{\mathrm{III}} - \dot{G}_{\phi,\mathrm{total}}^{\mathrm{II}} = \dot{Q}_{\mathrm{CW}}^{\mathrm{III}}\Delta T^{\mathrm{III}} - \dot{Q}_{\mathrm{CW}}^{\mathrm{II}}\Delta T^{\mathrm{II}} \tag{26}$$

where

$$\Delta T^{\mathrm{II}} = T_{\mathrm{FH}} - T_{\mathrm{CW}} + T_0 - T_1 \tag{27}$$

$$\Delta T^{\mathrm{III}} = \frac{T_2 + T_0}{2} - T_{\mathrm{CW}} \tag{28}$$

For practical chemical processes, $(T_2 - T_0)/2$ is much smaller than $T_{\mathrm{FH}} - T_1$, and thus $\Delta T^{\mathrm{III}} \ll \Delta T^{\mathrm{II}}$. Moreover, $\dot{Q}_{\mathrm{CW}}^{\mathrm{III}} < \dot{Q}_{\mathrm{CW}}^{\mathrm{II}}$ according to the energy relation $\dot{Q}_{\mathrm{CW}}^{\mathrm{II}} = \dot{Q}_{\mathrm{CW}}^{\mathrm{III}} = \dot{W}_{\mathrm{E}}$. As a consequence, we obtain $\dot{G}_{\phi,\mathrm{total}}^{\mathrm{III}} \ll \dot{G}_{\phi,\mathrm{total}}^{\mathrm{II}}$.

It is known that the introduction of a feed−effluent heat exchanger into a chemical process can improve the heat-transfer performance. Furthermore, a chemical process using SHRT has a better heat-transfer performance than a comparable process using a conventional heat-recovery approach. These improvements are essentially attributed to the decrease in the irreversible loss during heat-transfer processes. As the entransy-dissipation rate is a measurement of the irreversibility of a heat-transfer process with the purpose of pure object heating or cooling, the heat-transfer irreversibility characteristics of processes I−III can be compared graphically by the entransy-dissipation rates represented by the areas in the $T-\dot{Q}$ diagram, as illustrated in Figure 8. This comparison reveals that

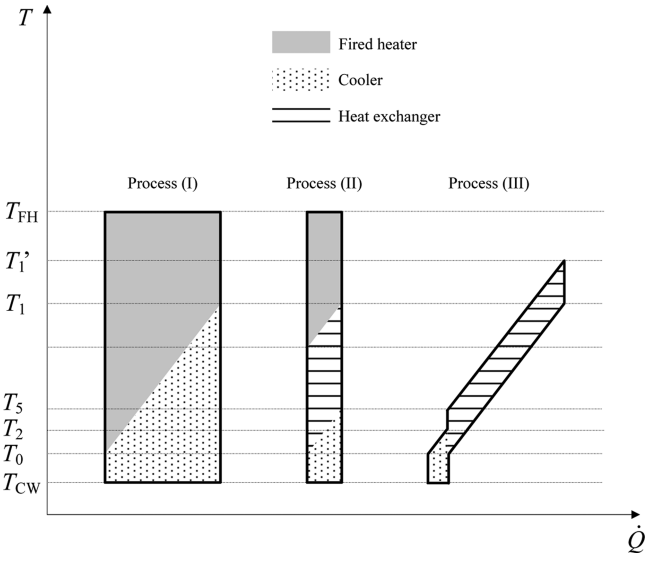

Figure 8. Comparison of the entransy-dissipation rates of processes I−III.

the low entransy-dissipation rate is the underlying mechanism for the good heat-transfer performance and the consequent significant energy savings of SHRT.

4.2. Vapor/Liquid Stream. Figure 9a shows simple chemical process IV for a vapor/liquid stream. The specific heat capacities of the liquid and vapor at constant pressure, $c_{p,l}$ and $c_{p,g}$, respectively, are assumed to be constant. A phase change from liquid to vapor occurs in the fired heater, and a change from vapor to liquid occurs in the cooling water cooler. The $T-\dot{Q}$ diagram of process IV, in which the shaded and patterned areas together represent the entransy-dissipation rate, is shown in Figure 9b. It can be seen that, without any heat recovery, the fired heater and cooler have to provide the whole heating and cooling load, where T_b stands for the boiling temperature of the stream at the operating pressure.

dx.doi.org/10.1021/ie4031506 | Ind. Eng. Chem. Res. XXXX, XXX, XXX−XXX

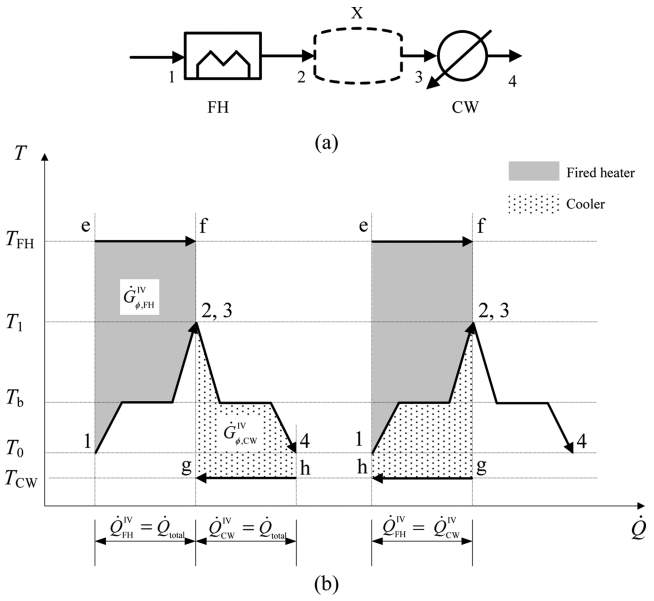

Figure 9. Simple thermal process IV for the vapor/liquid phase change stream: (a) flow diagram;[4] (b) $T-\dot{Q}$ diagram, where the shaded and patterned areas together represent the entransy-dissipation rate.

Assuming that the temperatures of the fired heater, T_{FH}, and cooling water, T_{CW}, remain constant during process 1−2 and 3−4, respectively, the total entransy-dissipation rate of process IV is the sum of $\dot{G}^{IV}_{\phi,FH}$ and $\dot{G}^{IV}_{\phi,CW}$ represented by the shaded and patterned areas, respectively, in Figure 9b with the expression

$$\dot{G}^{IV}_{\phi,total} = \dot{G}^{IV}_{\phi,FH} + \dot{G}^{IV}_{\phi,CW} = \dot{Q}_{total}(T_{FH} - T_{CW}) \quad (29)$$

which is just the area of the rectangle e−f−g−h shown in Figure 9b. Here, the letters e−h represent the four vertices of the rectangle. It can be found from eq 29 that the total entransy-dissipation rate of process IV is very large because T_{FH} is much higher than T_{CW}.

Improved chemical process V with a feed−effluent heat exchanger for the vapor/liquid stream is illustrated in Figure 10a, where only a small part of the latent heat in the phase change is recovered because of the finite temperature difference, ΔT_{min}, of the heat exchanger. As a result, the external heating and cooling loads, that is, the unrecovered latent heat and sensible heat, $\dot{Q}^{V}_{FH}$ and $\dot{Q}^{V}_{CW}$, respectively, are much larger than the self-heat duty $\dot{Q}^{V}_{HX}$.[4] Entransy dissipation occurs in the fired heater, the heat exchanger, and the cooler, as illustrated by the areas of the three polygons in Figure 10b, where $\dot{G}^{V}_{\phi,FH}$, $\dot{G}^{V}_{\phi,HX}$, and $\dot{G}^{V}_{\phi,CW}$ denote the entransy-dissipation rates of the heat-transfer processes occurring in these three pieces of equipment.

Calculations of the three areas give

$$\dot{G}^{V}_{\phi,FH} = (T_{FH} - T_b)\dot{Q}^{V}_{FH} - \frac{1}{2}\dot{m}c_{p,g}(T_1 - T_b)^2 \quad (30)$$

$$\dot{G}^{V}_{\phi,HX} = \frac{1}{2}\dot{m}c_{p,l}(T_b - T_0)^2 + \frac{1}{2}\dot{m}c_{p,g}(T_1 - T_b)^2 \quad (31)$$

and

$$\dot{G}^{V}_{\phi,CW} = (T_b - T_{CW})\dot{Q}^{V}_{CW} - \frac{1}{2}\dot{m}c_{p,l}(T_b - T_0)^2 \quad (32)$$

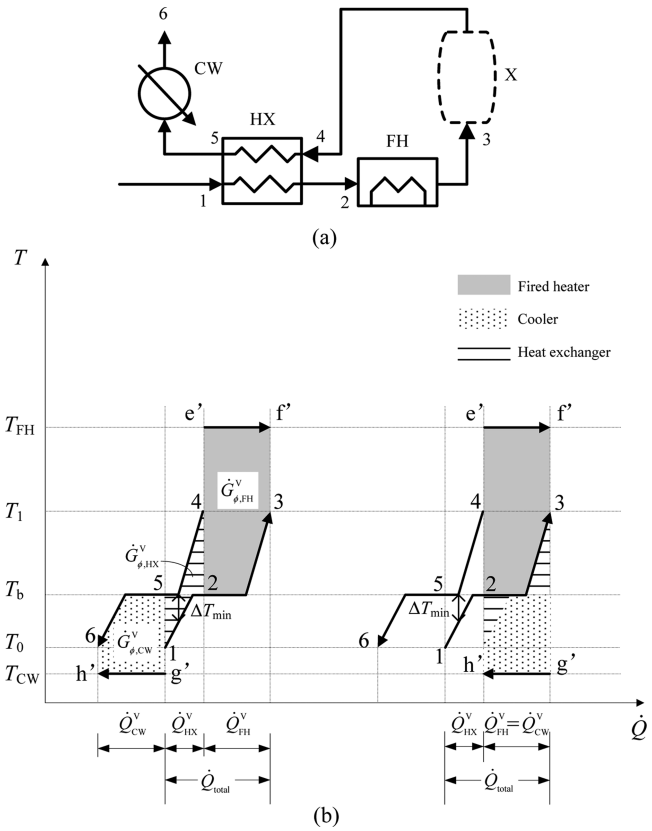

Figure 10. Improved thermal process V with a feed−effluent heat exchanger for the vapor/liquid phase change stream: (a) flow diagram;[4] (b) $T-\dot{Q}$ diagram, where the shaded and patterned areas together represent the entransy-dissipation rate.

where $\dot{Q}^{V}_{CW} = \dot{Q}^{V}_{FH}$. By adding the areas of the three polygons, one can obtain the total entransy-dissipation rate of process V as

$$\dot{G}^{V}_{\phi,total} = \dot{G}^{V}_{\phi,FH} + \dot{G}^{V}_{\phi,HX} + \dot{G}^{V}_{\phi,CW} = \dot{Q}^{V}_{FH}(T_{FH} - T_{CW}) \quad (33)$$

which just equals the area of rectangle e′−f′−g′−h′, as shown in Figure 10b. This result can also be obtained by a series of parallel movements of the areas because the curves of the feed and effluent streams in Figure 10b are symmetric.

Comparison of eqs 29 and 33 reveals that the entransy-dissipation rate of process V is lower than that of process IV because $\dot{Q}^{V}_{FH} < \dot{Q}_{total}$. However, the decrease in the entransy-dissipation rate (i.e., the decrease in the irreversibility) caused by the introduction of a feed−effluent heat exchanger is not remarkable because $\dot{Q}^{V}_{FH}$ is still large for process V.

Figure 11a shows thermal process VI for a vapor/liquid stream for heat circulation using SHRT.[4] Before entering the heat exchanger (HX), the effluent stream is compressed adiabatically by a compressor to a higher temperature, T_1'. Consequently, the total heating duty of the feed stream can be provided solely by the effluent stream with the self-heat exchanger. After that, the effluent stream from HX is depressurized by a valve (VL) and finally cooled to T_0 by releasing heat to the cooling water (CW).

The total entransy-dissipation rate of process VI can be represented by the sum of the two patterned areas in the $T-\dot{Q}$ diagram presented in Figure 11b, where $\dot{G}^{VI}_{\phi,HX}$ and $\dot{G}^{VI}_{\phi,CW}$ are the entransy-dissipation rates of the heat-transfer process

dx.doi.org/10.1021/ie4031506 | Ind. Eng. Chem. Res. XXXX, XXX, XXX−XXX

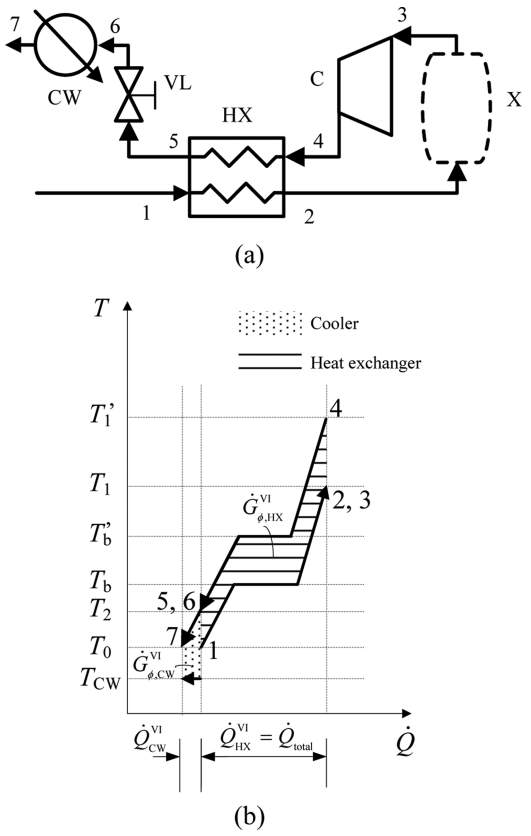

Figure 11. Thermal process VI with SHRT for the vapor/liquid phase change stream: (a) flow diagram;[4] (b) $T-\dot{Q}$ diagram, where the patterned areas together represent the entransy-dissipation rate.

between feed and effluent streams in the heat exchanger (HX) and that between effluent stream and the cooling water, respectively.

A comparison of entransy-dissipation rates among processes IV–VI is shown in Figure 12. It can be seen that the entransy dissipation of process V is lower than that of process IV because of the lower irreversibility of heat-transfer processes achieved by heat recovery. Nevertheless, because most of the latent heat of the phase change cannot be recovered by self-heat exchange, the entransy-dissipation rate of process V is still large. Using SHRT, however, in addition to the sensible heat, the latent heat is also circulated,[4] avoiding the large irreversible loss of the heat-transfer process in the fired heater due to the large temperature difference between the stream and the fuel. As a consequence, process VI has a much lower entransy-dissipation rate than processes IV and V, which can be intuitively seen from Figure 12. A further, more detailed quantitative analysis is presented in a case study in the next section.

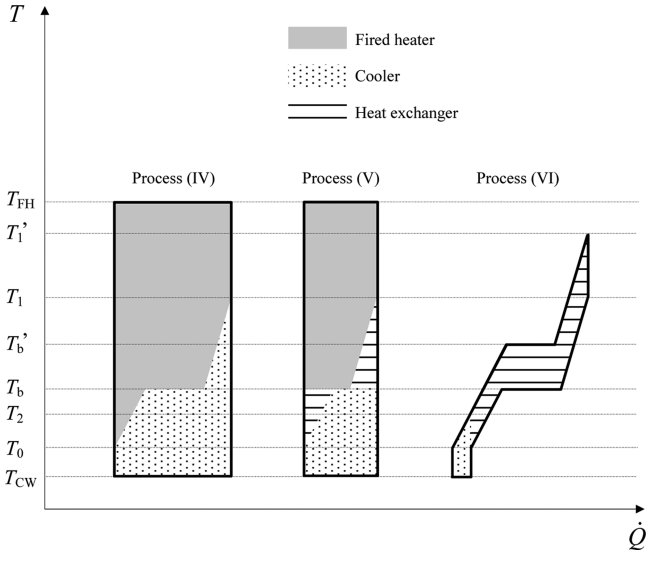

Figure 12. Comparison of the entransy-dissipation rates of processes IV–VI.

The extremum-entransy-dissipation principle indicates that, when the total heat exchange is prescribed, the lower the entransy dissipation, the better the heat-transfer performance. Under conditions of both gas streams and vapor/liquid streams as analyzed above, the total heat load $\dot{Q}_{total}$ is fixed, and it can be seen that the introduction of a compressor, which changes the pressure parameter of the stream, can dramatically decrease the entransy-dissipation rate of the thermal process, leading to greater heat recovery and/or lower external heating and cooling loads.

5. CASE STUDY AND DISCUSSION

In this section, we show the two cases of a gas stream and a vapor/liquid stream to further illustrate the feasibility of entransy analysis of self-heat recuperation technology based on heat-transfer irreversibility. For both cases, the stream is heated from T_0 = 300 K to a set temperature of T_1 = 500 K. The mass flow rate of the stream, $\dot{m}$, is set to 10 kg/s, and the minimum temperature difference, ΔT_{min}, is assumed to be 10 K. In addition, the temperatures of the fuel in the fired heater, T_{FH}, and the cooling water in the cooler, T_{CW}, are assumed to be 1100 and 290 K, respectively. There is no heat loss in the heat exchangers.

First, consider thermal processes II and III as shown in Figures 6a and 7a. Methane is used for the gas stream, and an average specific heat capacity at constant pressure within the temperature interval between 300 and 500 K of c_p = 2.58 kJ/(kg·K) is taken.

For process II, according to eqs 18–20, one can obtain the entransy-dissipation rates of the heat-transfer processes in the fired heater (FH), the feed–effluent heat exchanger (HX), and the cooling water cooler (CW) as shown in Table 1. The entransy-dissipation rate in FH is approximately three-quarters of the total entransy-dissipation rate, indicating that the irreversibility mainly occurs in the fired heater because of the very large temperature difference between the stream and the fuel in FH.

For process III, assuming that the expander recovers half of the shaft work of the compressor, we have T_2 = 305 K. Based on eqs 22 and 23, the entransy-dissipation rates of the heat-transfer processes in HX and CW can be derived and are also listed in Table 1. It can be seen from Table 1 that, because of the removal of the fired heater, the entransy-dissipation rate of process III with SHRT is only one-fourth that of conventional self-heat exchange thermal process II. From the point of view of energy, the energy requirement of process III is one-half that of process II.

The second case is for a vapor/liquid stream with water used as the working fluid. Consider thermal processes V and VI as shown in Figures 10a and 11a. The boiling point, T_b, is set to 373 K, and the latent heat of vaporization of water is γ = 2258 kJ/kg. We assume that the specific heat capacities at constant

dx.doi.org/10.1021/ie4031506 | Ind. Eng. Chem. Res. XXXX, XXX, XXX–XXX

Table 1. Entransy-Dissipation Rates and Energy Requirements of Conventional Thermal Process II and the Process with SHRT for the Gas Stream (Process III)

	entransy-dissipation rate (MW·K)				energy requirement (kW)		
process	fired heater	feed−effluent heat exchanger	cooler	total	fired heater	compressor and expander ($\dot{W}_c - \dot{W}_E$)	total
II	156.09	49.02	3.87	208.98 (100%)	258	–	258 (100%)
III	–	51.60	1.61	53.21 (25%)	–	129	129 (50%)

Table 2. Entransy-Dissipation Rates and Energy Requirements of Conventional Thermal Process V and the Process with SHRT for the Vapor/Liquid Stream (Process VI)

	entransy-dissipation rate (MW·K)				energy requirement (kW)		
process	fired heater	feed−effluent heat exchanger	cooler	total	fired heater	compressor ($\dot{W}_c$)	total
V	16545.17	267.87	1800.76	18613.80 (100%)	22980	–	22980 (100%)
VI	–	418.45	6.00	424.45 (2.2%)	–	400	400 (1.7%)

pressure of the vapor and liquid, $c_{p,g}$ and $c_{p,l}$, are approximately 4 and 2 kJ/(kg·K), respectively, during processes V and VI.

The self-heat-exchange load and the total heat duty of process V as shown in Figure 10b can be calculated as

$$\dot{Q}_{HX}^{V} = \dot{m}c_{p,l}(T_b - T_0 - \Delta T_{min}) + \dot{m}c_{p,g}(T_1 - T_b) \quad (34)$$

and

$$\dot{Q}_{total} = \dot{m}c_{p,l}(T_b - T_0) + \dot{m}c_{p,g}(T_1 - T_b) + \dot{m}\gamma \quad (35)$$

Based on eqs 34 and 35, the external heating load, $\dot{Q}_{FH}^{V}$, is

$$\dot{Q}_{FH}^{V} = \dot{Q}_{total} - \dot{Q}_{HX}^{V} = \dot{m}c_{p,l}\Delta T_{min} + \dot{m}\gamma \quad (36)$$

Substituting the given values of the parameters into eq 36 yields $\dot{Q}_{FH}^{V}$ = 22.98 MW.

Further, based on eqs 30−32, the entransy-dissipation rates $\dot{G}_{\phi,FH}^{V}$, $\dot{G}_{\phi,HX}^{V}$, and $\dot{G}_{\phi,CW}^{V}$ can be obtained as shown in Table 2, where the entransy-dissipation rate in FH is approximately nine-tenths of the total, showing once again that the irreversible loss is mostly attributable to the large temperature difference of the heat-transfer process between the stream and the fuel in FH.

For process VI, the boiling temperature at a higher pressure, T_b', is shifted to 388 K, 15 K higher than T_b, as shown in Figure 13. The entransy-dissipation rates of heat transfer in CW and HX are represented by the areas of trapezoid a−b−6−7 and polygon 1−c−f−2−4−h−i−6, respectively. The area of trapezoid a−b−6−7 is given by

$$A_{a-b-6-7} = \frac{(T_0 - T_{CW} + T_2 - T_{CW})}{2}\dot{Q}_{CW}^{VI} \quad (37)$$

where $T_2 = T_0 + \Delta T_{min}$ and $\dot{Q}_{CW}^{VI} = \dot{m}c_{p,l}\Delta T_{min}$.

Similarly, the areas of trapezoids c−d−i−j and e−f−g−h can be expressed as

$$A_{c-d-i-j} = \frac{(\Delta T_{min} + T_b' - T_b)}{2}\dot{m}c_{p,l}(T_b' - T_b - \Delta T_{min}) \quad (38)$$

and

$$A_{e-f-g-h} = \frac{(T_b' - T_b + T_1' - T_1)}{2}\dot{m}c_{p,g}[(T_1' - T_1) - (T_b' - T_b)] \quad (39)$$

Meanwhile, the areas of the three parallelograms are given by

$$A_{1-c-j-6} = \Delta T_{min}\dot{m}c_{p,l}(T_b - T_0) \quad (40)$$

$$A_{d-e-h-i} = (T_b' - T_b)[\dot{m}\gamma - \dot{m}c_{p,l}(T_b' - T_b - \Delta T_{min}) - \dot{m}c_{p,g}(T_1' - T_1 - T_b' + T_b)] \quad (41)$$

and

$$A_{f-2-4-g} = (T_1' - T_1)\dot{m}c_{p,g}(T_1 - T_b) \quad (42)$$

By adding eqs 38−42, one can obtain the entransy-dissipation rate of heat transfer in HX.

The unknown values of T_1' in eqs 38−42 can be derived as follows: In process VI, the enthalpy change of the vapor during process 3−4 is equal to that of the liquid during process 6−7 according to the law of energy conservation, that is

$$\dot{m}c_{p,g}(T_1' - T_1) = \dot{m}c_{p,l}\Delta T_{min} \quad (43)$$

Thus, we have

$$T_1' = \frac{c_{p,l}}{c_{p,g}}\Delta T_{min} + T_1 \quad (44)$$

With the given parameters, we obtain T_1' = 520 K.

The total entransy-dissipation rate for process VI shown in Table 2 is dramatically reduced because of the removal of the fired heater. Moreover, because the thermal process with SHRT recovers all the latent heat of the stream, the entransy-dissipation rate of the heat transfer in CW is also reduced

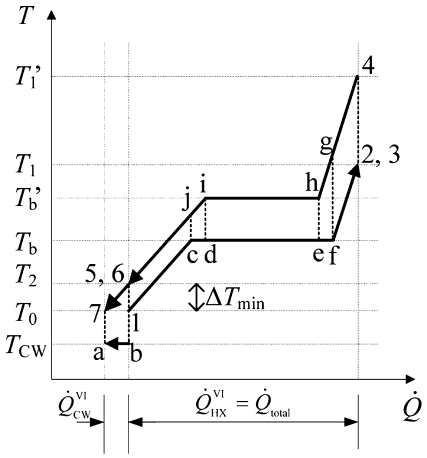

Figure 13. Schematic $T-\dot{Q}$ diagram for the calculation of the entransy-dissipation rate of process VI.

dx.doi.org/10.1021/ie4031506 | Ind. Eng. Chem. Res. XXXX, XXX, XXX−XXX

Table 3. Exergy-Destruction Rates and Energy Requirements of Conventional Thermal Process II and the Process with SHRT for the Gas Stream (Process III) (T_0 = 25 °C)

	exergy-destruction rate (kW)				energy requirement (kW)		
process	fired heater	feed−effluent heat exchanger	cooler	total	fired heater	compressor and expander	total
II	85.44	96.77	13.01	195.22 (100%)	258	–	258 (100%)
III	–	99.85	5.47	105.32 (54%)	–	129	129 (50%)

Table 4. Exergy-Destruction Rates and Energy Requirements of Conventional Thermal Process V and the Process with SHRT for the Vapor/Liquid Stream (Process VI) (T_0 = 25 °C)

	exergy-destruction rate (kW)				energy requirement (kW)		
process	fired heater	feed−effluent heat exchanger	cooler	total	fired heater	compressor	total
V	11851.04	546.07	4991.31	17388.42 (100%)	22980	–	22980 (100%)
VI	–	849.95	20.18	870.13 (5.0%)	–	400	400 (1.7%)

greatly. As a result, the total entransy-dissipation rate of the process VI with SHRT is only 1/44 that of the conventional self-heat-exchange thermal process V. The energy requirement of process VI is approximately 1.7% of that of process V only.

In previous studies, the irreversibility of a thermal process with heat circulation using SHRT was analyzed on the basis of exergy destruction.[3] Neglecting the flowing resistance, the exergy-destruction rate due to heat transfer between the hot and cold fluids in a heat exchanger is

$$\dot{I} = \dot{Q}T_0\left(\frac{1}{\overline{T}_c} - \frac{1}{\overline{T}_h}\right) \tag{45}$$

where $\dot{Q}$ is the total heat-transfer rate in the heat exchanger, and

$$\overline{T}_c = \frac{T_{c,out} - T_{c,in}}{\ln\frac{T_{c,out}}{T_{c,in}}}, \quad \overline{T}_h = \frac{T_{h,in} - T_{h,out}}{\ln\frac{T_{h,in}}{T_{h,out}}} \tag{46}$$

For the two cases of gas and vapor/liquid streams with the values of parameters as presented above, the exergy-destruction rates of the heat-transfer processes in the fired heater (FH), feed−effluent heat exchanger (HX), and cooler (CW) are obtained as reported in Tables 3 and 4, respectively. It can be seen that the exergy-destruction rates of the thermal processes with SHRT are dramatically reduced compared with those of the corresponding conventional self-heat-exchange thermal processes.

Although the results based on the exergy analysis shown in Tables 3 and 4 have the same trends as those derived from the entransy analysis shown in Tables 1 and 2, respectively, there are important differences between these two analysis methods. First, unlike the exergy-destruction rate, the entransy-dissipation rate of a thermal process can be graphically represented by the area between the lines of the hot and cold fluids in the $T-\dot{Q}$ diagram, providing a convenient approach to compare the irreversibility of an advanced process using SHRT with that of a conventional self-heat-exchange thermal process. Second, in exergy analysis, the choice of the environmental temperature, T_0, is arbitrary to some extent. Consequently, different choices of T_0 will result in different exergy-destruction rates for a given thermal process, as shown in Table 5. The value of the entransy-dissipation rate, however, is independent of T_0, and there is a unique value of entransy-dissipation rate for each given thermal process. This is because, for the concept of exergy, the reference point is the state in thermodynamic equilibrium with the environment, whereas for the concept of entransy, according to its definition,[10] the reference point is a temperature of absolute zero. Third, previous studies have shown that the minimum exergy-destruction rate does not correspond to the maximum heat-transfer rate between hot and cold fluids when a heat-transfer process is for the purpose of pure object heating or cooling.[12,32,33] Hence, for the analysis of optimization problems of heat-transfer processes using SHRT whose purpose is object heating or cooling rather than heat−work conversion, the entransy analysis might be more appropriate. Research in this area is still in progress.

Table 5. Exergy-Destruction Rates (kW) of Process VI for Different Environmental Temperatures

environmental temperature (°C)	fired heater	feed−effluent heat exchanger	cooler	total
20	–	835.69	19.84	855.53
25	–	849.95	20.18	870.13
30	–	864.21	20.52	884.73

6. CONCLUSIONS

Heat-transfer processes can be divided into two categories depending on their purpose. When the transferred heat is for heat−work conversion, the exergy-destruction rate is the appropriate measure of irreversibility, and optimization should involve application of the exergy-destruction principle. In contrast, when the transferred heat is for object heating or cooling only, the entransy-dissipation rate is the appropriate measure of irreversibility, and the entransy-dissipation principle should be applied for optimization of the global heat-transfer performance. In view of the fact that the objective of heat-transfer processes in SHRT is to heat or cool streams only, entransy analysis should be applied to evaluate the performance of SHRT.

A temperature−heat-flow-rate diagram ($T-\dot{Q}$ diagram) can be applied to describe heat-transfer irreversibility graphically and quantitatively. The $T-\dot{Q}$ diagram used in entransy analysis is different from that used in both pinch technology and SHRT. First, the area between the lines of the hot and cold fluids with the physical meaning of the entransy-dissipation rate can be used to evaluate the performance of SHRT. Second, unlike in pinch technology, the lines of the hot and cold fluids in the $T-\dot{Q}$ diagram for irreversibility analysis cannot be added together because the area between the composite curves is no longer the entransy-dissipation rate of the multistream heat-exchange process.

dx.doi.org/10.1021/ie4031506 | Ind. Eng. Chem. Res. XXXX, XXX, XXX−XXX

Both entransy analyses in terms of temperature−heat-flow-rate diagrams and exergy analyses indicate that, compared to conventional self-heat-exchange processes, much greater heat recovery and much lower energy requirements can be attributed to much lower entransy dissipation or exergy destruction for SHRT as a result of changing the pressure of the effluent stream with a compressor. However, for the performance analysis of SHRT, exergy analysis has some disadvantages, including arbitrary values of exergy-destruction rates due to the arbitrary choice of reference point and no graphical plot of the exergy-destruction rate.

AUTHOR INFORMATION

Corresponding Author

*E-mail: jingwu12@gmail.com.

Notes

The authors declare no competing financial interest.

ACKNOWLEDGMENTS

This research was supported by the National Natural Science Foundation of China (51206079).

REFERENCES

(1) Linnhoff, B. Pinch analysis—A state-of-the-art overview. *Trans. Inst. Chem. Eng.* **1993**, *71* (A5), 503−522.

(2) Linnhoff, B.; Hindmarsh, E. The pinch design method of heat exchanger networks. *Chem. Eng. Sci.* **1983**, *38*, 745−763.

(3) Matsuda, K.; Kawazuishi, K.; Hirochi, Y.; Sato, R.; Kansha, Y.; Fushimi, C.; Shikatani, Y.; Kunikiyo, H.; Tsutsumi, A. Advanced energy saving in the reaction section of the hydro-desufurization process with self-heat recuperation technology. *Appl. Therm. Eng.* **2010**, *30*, 2300−2305.

(4) Kansha, Y.; Tsuru, N.; Sato, K.; Fushimi, C.; Tsutsumi, A. Self-Heat Recuperation Technology for Energy Saving in Chemical Processes. *Ind. Eng. Chem. Res.* **2009**, *48*, 7682−7686.

(5) Kansha, Y.; Tsuru, N.; Fushimi, C.; Tsutsumi, A. Integrated process module for distillation processes based on self-heat recuperation technology. *J. Chem. Eng. Jpn.* **2010**, *43*, 502−507.

(6) Kansha, Y.; Tsuru, N.; Fushimi, C.; Tsutsumi, A. New design methodology based on self-heat recuperation for production by azeotropic distillation. *Energy Fuels* **2010**, *24*, 6099−6102.

(7) Aziz, M.; Fushimi, C.; Kansha, Y.; Mochidzuki, K.; Kaneko, S.; Tsutsumi, A.; Matsumoto, K.; Hashimoto, T.; Kawamoto, N.; Oura, K.; Yokohama, K.; Yamaguchi, Y.; Kinoshita, M. Innovative energy-efficient biomass drying based on self-heat recuperation technology. *Chem. Eng. Technol.* **2011**, *34*, 1095−1103.

(8) Aziz, M.; Kansha, Y.; Tsutsumi, A. Self heat recuperative fluidized bed drying of brown coal. *Chem. Eng. Process.* **2011**, *50*, 944−951.

(9) Kishimoto, A.; Kansha, Y.; Fushimi, C.; Tsutsumi, A. Exergy Recuperative CO_2 Gas Separation in Post-Combustion Capture. *Ind. Eng. Chem. Res.* **2011**, *50*, 10128−10135.

(10) Guo, Z. Y.; Zhu, H. Y.; Liang, X. G. Entransy−A physical quantity describing heat transfer ability. *Int. J. Heat Mass Transfer* **2007**, *50*, 2545−2556.

(11) Chen, Q.; Zhu, H. Y.; Pan, N.; Guo, Z.-Y. An alternative criterion in heat transfer optimization. *Proc. R. Soc. A: Math. Phys. Eng. Sci.* **2011**, *467*, 1012−1028.

(12) Chen, Q.; Wu, J.; Wang, M. R.; Pan, N.; Guo, Z.-Y. A comparison of optimization theories for energy conservation in heat exchager groups. *Chin. Sci. Bull.* **2011**, *56*, 449−454.

(13) Chen, Q.; Wang, M. R.; Pan, N.; Guo, Z.-Y. Optimization principles for convective heat transfer. *Energy* **2009**, *34*, 1199−1206.

(14) Chen, Q.; Liang, X. G.; Guo, Z. Y. Entransy theory for the optimization of heat transfer—A review and update. *Int. J. Heat Mass Transfer* **2013**, *63*, 65−81.

(15) Bejan, A. A study of entropy generation in fundamental convective heat transfer. *J. Heat Transfer ASME* **1979**, *101*, 718−725.

(16) Bejan, A. Entropy generation minimization: The new thermodynamics of finite-size devices and finite-time processes. *J. Appl. Phys.* **1996**, *79*, 1191−1218.

(17) Lerou, P. P. P. M.; Veenstra, T. T.; Burger, J. F.; ter Brake, H. J. M.; Rogalla, H. Optimization of counterflow heat exchanger geometry through minimization of entropy generation. *Cryogenics* **2005**, *45*, 659−669.

(18) Ko, T. H. A numerical study on entropy generation and optimization for laminar forced convection in a rectangular curved duct with longitudinal ribs. *Int. J. Therm. Sci.* **2006**, *45*, 1113−1125.

(19) Andresen, B.; Gordon, J. M. Optimal paths for minimizing entropy generation in a common class of finite-time heating and cooling processes. *Int. J. Heat Fluid Flow* **1992**, *13*, 294−299.

(20) Caldas, M.; Semiao, V. Entropy generation through radiative transfer in participating media: Analysis and numerical computation. *J. Quant. Spectrosc. Radiat. Transfer* **2005**, *96*, 423−437.

(21) Bertola, V.; Cafaro, E. A critical analysis of the minimum entropy production theorem and its application to heat and fluid flow. *Int. J. Heat Mass Transfer* **2008**, *51*, 1907−1912.

(22) Finlayson, B. A., Ed. *The Method of Weighted Residuals and Variational Principles: With Application in Fluid Mechanics, Heat and Mass Transfer*; Mathematics in Science and Engineering Series; Academic Press: New York, 1972; Vol. *87*.

(23) Hesselgreaves, J. E. Rationalisation of second law analysis of heat exchangers. *Int. J. Heat Mass Transfer* **2000**, *43*, 4189−4204.

(24) Shah, R. K.; Skiepko, T. Entropy generation extrema and their relationship with heat exchanger effectiveness—Number of transfer unit behavior for complex flow arrangements. *J. Heat Transfer ASME* **2004**, *126*, 994−1002.

(25) Guo, Z. Y.; Cheng, X. G.; Xia, Z. Z. Least dissipation principle of heat transport potential capacity and its application in heat conduction optimization. *Chin. Sci. Bull.* **2003**, *48*, 406−410.

(26) Guo, Z. Y.; Liu, X. B.; Tao, W. Q.; Shah, R. K. Effectiveness−thermal resistance method for heat exchanger design and analysis. *Int. J. Heat Mass Transfer* **2010**, *53*, 2877−2884.

(27) Cheng, X. T.; Wang, W. H.; Liang, X. G. Entransy analysis of open thermodynamic systems. *Chin. Sci. Bull.* **2012**, *57*, 2934−2940.

(28) Xia, S. J.; Chen, L. G.; Sun, F. R. Entransy dissipation minimization for liquid−solid phase processes. *Sci. China: Technol. Sci.* **2010**, *53*, 960−968.

(29) Xia, S J; Chen, L G; Sun, F R. Optimization for entransy dissipation minimization in heat exchanger. *Chin. Sci. Bull.* **2009**, *54*, 3587−3595.

(30) Chen, Q.; Xu, Y. C.; Guo, Z. Y. The property diagram in heat transfer and its applications. *Chin. Sci. Bull.* **2012**, *57*, 4646−4652.

(31) Kemp, I. C. *Pinch Analysis and Process Integration: A User Guide on Process Integration for the Efficient Use of Energy*, 2nd ed.; Butterworth-Heinemann: Oxford, U.K., 2007; pp 16−21.

(32) Chen, L.; Chen, Q.; Li, Z.; Guo, Z.-Y. Optimization for a heat exchanger couple based on the minimum thermal resistance principle. *Int. J. Heat Mass Transfer* **2009**, *52*, 4778−4784.

(33) Liu, X. B.; Meng, J. A.; Guo, Z. Y. Entropy generation extremum and entransy dissipation extremum for heat exchanger optimization. *Chin. Sci. Bull.* **2009**, *54*, 943−947.